Sciencexpress Report

Trace Metals as Biomarkers for Eumelanin Pigment in the Fossil Record

R. A. Wogelius,[1,2*] P. L. Manning,[1,2,3] H. E. Barden,[1,2] N. P. Edwards,[1,2] S. M. Webb,[4] W. I. Sellers,[5] K. G. Taylor,[6] P. L. Larson,[1,7] P. Dodson,[3,8] H. You,[9] L. Da-qing,[10] U. Bergmann[11]

[1]University of Manchester, School of Earth, Atmospheric, and Environmental Sciences, Manchester M13 9PL, UK. [2]University of Manchester, Williamson Research Centre for Molecular Environmental Science, Manchester M13 9PL, UK. [3]University of Pennsylvania, Department of Earth and Environmental Sciences, Philadelphia, PA 19104, USA. [4]Stanford Synchrotron Radiation Lightsource, SLAC National Accelerator Laboratory, Menlo Park, CA 94025, USA. [5]University of Manchester, Faculty of Life Sciences, Manchester M13 9PT, UK. [6]School of Science and the Environment, Manchester Metropolitan University, Manchester M1 5GD, UK. [7]Black Hills Institute of Geological Research, Inc., Hill City, SD 57745, USA. [8]University of Pennsylvania, School of Veterinary Medicine, Philadelphia, PA 19104, USA. [9]Institute of Geology, Chinese Academy of Geological Sciences, 26 Baiwanzhuang Road, Beijing, P. R. China, 100037. [10]Gansu Geological Museum, 6 Tuan Jie Road, Lanzhou, Gansu, P. R. China, 730030. [11] Linac Coherent Light Source, SLAC National Accelerator Laboratory, Menlo Park, CA 94025, USA.

*To whom correspondence should be addressed. E-mail: roy.wogelius@manchester.ac.uk

Well-preserved fossils of pivotal early bird and non-avian theropod species have provided unequivocal evidence for feathers and/or down-like integuments. Recent studies have reconstructed color based upon melanosome structure; however, the chemistry of these proposed melanosomes has remained unknown. Here we apply synchrotron X-ray techniques to several fossil and extant organisms, including *Confuciusornis sanctus*, to map and characterize possible chemical residues of melanin pigments. Results show that trace metals, such as copper, are present in fossils as organometallic compounds most likely derived from original eumelanin. The distribution of these compounds provides a long-lived biomarker of melanin presence and density within a range of fossilized organisms. Metal zoning patterns may be preserved long after melanosome structures have been destroyed.

Feather color in birds stems mostly from chemical pigments, of which the most widely used are melanins (*1*). Resolving color patterns in extinct species may hold the key to understanding selection processes that acted during crucial evolutionary periods and also may help discern non-flight functions such as camouflage, communication, and sexual selection.

Confuciusornis sanctus (Jehol Group, Lower Cretaceous, 131-120 Ma) and *Gansus yumenensis* (Xiagou Formation, Lower Cretaceous, 115-105 Ma) occupy key positions in the evolution of Aves; *C. sanctus* is the oldest documented species to display the derived avian beak (*2*) and *G. yumenensis* has been identified as the most ancient of the Ornithurae, the phylogenetic grouping which includes modern birds (*3*). Previous studies of similar material (*4*, *5*) suggested the presence of melanosomes and tentatively reconstructed feather colors. These studies used melanosome shape to extrapolate color; rod shapes were interpreted as eumelanosomes (dark black/brown) and spheroidal shapes as pheomelanosomes (reddish-brown). Other pigments (e.g. carotenoids) in feathers and physical structures besides melanosomes may contribute to color. Melanin granule morphology may vary among different species (*6*, *7*), and structural preservation may not be uniform. Therefore color interpretation based solely on fossilized melanosome morphology and distribution has limitations (*4*, *5*, *8*).

Despite these additional complicating factors in color restoration, detailed chemical analysis of fossil material may make it possible to resolve remnants of pigmentation. In particular, a number of biologically important metal ions (e.g., Ca^{2+}, Cu^{2+}, Co^{2+} and Zn^{2+}) are chelated by and affect the chemical properties of melanin (*1*, *9–11*) such that trace metal distributions are able to provide a chemical image of melanin distribution in extant feathers (*12*). Therefore, due to their non-biodegradability and the biocide properties of some metals this may also be the case in fossils. Assuming trace metal distributions correlate with proposed melanosomes, then a true chemical test would be to determine whether organic compounds (especially organo-metallic chelates) with an affinity to precursor melanin can be identified.

Here we apply chemical imaging to search for trace metal patterns in an exceptionally preserved specimen of *C. sanctus* (MGSF315), a lone feather of *G. yumenensis* (MGSF317), and several comparable fossil and extant samples including the holotype of *Archaeopteryx lithographica* (*13*). Chemical analysis of fossils without destructive sampling is

challenging, but recently Synchrotron Rapid Scanning X-Ray Fluorescence (SRS-XRF) has been successfully developed to fully map trace element distributions in large specimens that could not be observed with traditional methods (*14*). Extended X-ray Absorption Fine Structure (EXAFS) and X-ray Absorption Near Edge Structure (XANES) spectroscopies are used to probe the local structure of the mapped trace metals to determine whether they are likely to be derived from endogenous organic compounds. Variable Pressure-Field Emission Gun-Scanning Electron Microscopy (VP-FEG-SEM) is used to compare trace element maps to fossil microstructure and infra-red spectroscopy is used to corroborate the EXAFS and XANES.

SRS-XRF maps of *C. sanctus* specimen MGSF315 (Fig. 1A) and its counterpart reveal several correlations between chemical distributions and structural features. False color SRS-XRF images of Cu, Ca, and Zn data show that Cu is distinctly concentrated within the downy body feathers and also appears as discrete elongated patches within areas of the flight feathers (Fig. 1B). The characteristic *C. sanctus* retrices (tail feathers) can also be resolved in the copper map. Calcium (blue) is high in bone, as would be expected, and zinc (green) is distributed throughout the sedimentary rock at levels higher than copper. The counterpart slab mirrors the zonation pattern, indicating that the mapped metal distributions are reproducible and, more importantly, that the Cu distribution shown in Fig. 1B is not a partial chemical remnant caused by unevenly splitting the Cu inventory between two opposite slabs. A second *C. sanctus* specimen (LL12418) was mapped via SRS-XRF and also showed high Cu in the neck feathers (Fig. 1D). In birds which produce melanin, keratin may apparently chelate available copper (*15*) or traces of tyrosinase may be entrained during feather growth such that copper alone, despite its strong association with melanin production, should not solely be relied upon as an indicator of melanin-based pigmentation. Calcium, Zn, Fe, and Mn are also typically associated with melanin pigmentation (*12*, *16*). SRS-XRF maps of Ca (Fig. 1E) and Zn (Fig. 1F) in the downy feathers of the *C. sanctus* (MGSF315) neck region show strong correlations with Cu and with each other (figs. S1-S3, table S1). Sulfur is a major component of feathers (approx. 7 wt. %) and sulfur maps also correlate with divalent trace metals (Fig. 1G). Fe and Mn concentrations are so high in the sedimentary matrix that they obscure any patterning that might be present in the feather regions; however, the observed correlation of Cu, Ca, and Zn within S-bearing soft tissue regions implies that there is a melanin-chelate derived control on trace metal distribution in *C. sanctus* feathers.

VP-FEG-SEM imaging and chemical analysis of three ~1mm sized flakes from the counterpart of MGSF315 was completed to enable comparison of our synchrotron elemental mapping results to recent studies that have reconstructed pigmentation based on structural analysis of proposed fossilized melanosomes. The copper-rich neck sample showed some areas with elongate structures (Fig. 1H) that have been identified as fossilized eumelanosomes (*4*, *5*). The proximal flight feathers also showed these structures (fig. S4). Contrary to (*5*) we found no evidence of equant pheomelanosome structures in MGSF315 (or any other fossil) and so our results from this study pertain only to eumelanin. The sample taken from distal flight feathers with low copper showed no structures that could be interpreted as melanosomes.

As shown in our elemental maps, copper and other elements correlate with both macroscopic feather outlines and microscopic eumelanosome structures. These elements are either original to these fossils and reflect similar pigmentation in both of these specimens from the same taxa, or geochemical/geomicrobiological processes have acted posthumously on both, adding metals only to the feathers and preserving details of body and flight feathers.

Chemical spectroscopy suggests the patterning is likely endogenous. EXAFS analyses of copper oxide and copper melanin standards are compared to the flake sampled from the *C. sanctus* neck region and to a second fossil feather (BHI-6358) with high copper zones (Fig. 2A). The strong backscattering from ordered second shell (and more distant) copper atoms, which is diagnostic of copper oxide, is not present in the fossil feathers (figs. S5-S8, table S2). The radial distribution functions for *C. sanctus* and BHI-6358 are also inconsistent with other possible inorganic copper phases such as malachite [$Cu_2(OH)_2CO_3$; (*17*)], $Cu(OH)_2$ (*18*), or chalcopyrite [$CuFeS_2$; (*19*)]. In fact the Cu-coordination chemistry in both fossils is predominantly an organic molecular compound (Fig. 2B) with coordination chemistry similar to Cu in natural eumelanin. The planar atoms of the *C. sanctus* copper coordination complex superimposed onto a recently optimized computational model of melanin (*20*) also indicates that the EXAFS data are consistent with Cu being sequestered within the channels of eumelanin or melanin derived organic compounds (Fig. 2C). Copper bridging the edge carboxyl groups of two eumelanin fragments would also satisfy the EXAFS data (*21*). Thus the trace metal detail shown in Fig. 1 is most likely derived from original eumelanin chelates in the feathers (SOM Text, fig. S9, tables S3 and S4). Note that unlike the *C. sanctus* feathers, BHI-6358 did not show melanosome-like structures via VP-FEG-SEM analysis. However, high resolution XRF maps of BHI-6358 do show that copper enriched areas are aggregates of discrete patches 2 to 3 μm in size, consistent with original eumelanosome dimensions (figs. S4 and S10).

A range of additional fossil and extant organisms representing different geological conditions and various soft

tissue types were analyzed to test and constrain the *C. sanctus* results. Copper levels are elevated within the visibly darker regions of two Green River feathers (Fig. 3H and I). Although BHI-6358 did not preserve any detectable melanosomes, SEM analysis did reveal fossilized eumelanosomes within copper enriched areas of the feather exposed within BHI-6319 (fig. S4). The eye of the fossil fish in specimen BHI-6319 also shows elevated Cu levels (Fig. 3J) but traces of melanosomes in the fish eye could not be resolved. Eyes in extant fish have been shown to contain high concentrations of melanin-related copper (*22*). A lone *Gansus yumenensis* feather (MGSF317) displays areas of elevated trace copper (Fig. 3K) and these areas are correlated with preserved eumelanosome structures (fig. S4). Crucially, SRS-XRF maps of extant feathers show a correlation between pigment density and trace copper (Fig. 3L and M). Finally, results from both fossil (Fig. 3N) and extant squid (Fig. 3O) show that high copper concentrations correlate with the eumelanin-rich ink sack regions (*23*, *24*). All these maps are consistent with the proposed spatial correlation between original eumelanin pigmentation and copper.

XANES spectra, which are sensitive to the electronic structure of the probed central absorber atom, were acquired from several standards and fossil specimens. Three Green River feather specimens, a fossil squid, and the *C. sanctus* fossil all produced Cu XANES spectra that resemble the extant *Sepia officinalis* eumelanin standard (Fig. 4). This also holds for the Cu XANES taken from the holotype of *Archaeopteryx lithographica*, suggesting that the residue of melanin pigmentation patterns is present even within one of the earliest avian ancestors. Linear combination shows that organic complexes represent the majority of the copper inventory in all these fossils (Fig. 4; figs. S11 and S12, table S5). These results agree with the Cu/melanin correlation observed in *C. sanctus* and suggest that trace element chemistry provides a robust and consistent method for identifying pigment because metal zoning may be preserved long after melanosome structures have been destroyed, as in BHI-6358. Additionally, infra-red spectral analysis shows that the organic functional groups in *C. sanctus*, BHI-6358, and several of the other fossil feathers have a strong eumelanin affinity and a distribution pattern that is controlled by soft tissue residue, similar to recent results with fossil skin (*25*), figs. S13-S15, table S6).

Trace metals in *C. sanctus* are high in the downy feathers. Metal concentrations gradationally reduce within the proximal flight feathers but show patchy regions of higher concentration near the tips, indicating lighter bands in the proximal flight feathers. A lack of trace-metals in the distal flight feathers suggests these were not eumelanin-rich and the lack of preserved melanosomes argues against pheomelanosome pigmentation. Distal flight feathers therefore were either mostly white or colored by another mechanism, such as carotenoids. This suggests that *Confuciusornis sanctus* most probably had darkly shaded regions, with the most intense eumelanin pigmentation in the downy body feathers and in the lengthy retrices (see Fig. 1-I).

References and Notes

1. J. D. Simon, D. Peles, K. Wakamatsu, S. Ito. *Pigment Cell Melanoma Res.* **22**, 563-579 (2009).
2. L.H. Hou, L. D. Martin, Z.H. Zhou, A. Feduccia, F.C. Zhang. *Nature* **399**, 679-682 (1999).
3. H. L. You *et al.*, *Science* **312**, 1640-1643 (2006).
4. F. C. Zhang *et al.*, *Nature* **463**, 1075-1078 (2010).
5. Q. Li *et al.*, *Science* **327**, 1369-1372 (2010).
6. B. H. Willier, M. E. Rawles, *Physiol. Zool*. **13**, 177-201 (1940).
7. C. L. Ralph, *Am. Zool.* **9**, 521-530 (1969).
8. J. A. Clarke *et al.*, *Science* **330**, 954-957 (2010).
9. A. Palumbo, M. Dischia, G. Misuraca, G. Prota, T. M. Schultz, *Biochim. Biophys. Acta* **964**, 193-199 (1988).
10. B. S. Larsson, *Pigment Cell Res.* **6**, 127-133 (1993).
11. K. J. McGraw, *Oikos* **102**, 402-406 (2003).
12. M. Niecke, M. Heid, A. Kruger, *J. Ornithology* **140** (3), 355-362 (1999).
13. Materials and Methods are available on *Science* Online.
14. U. Bergmann *et al.*, *Proc. Natl. Acad. Sci. U.S.A.* **107** (20), 9060-9065 (2010).
15. M. Katsikini, E. Mavromati, F. Pinakidou, E.C. Paloura, D. Gioulekas, *J. Phys.: Conf. Ser.* **190**, 012204 (2009)
16. K. J. McGraw, in *Bird Coloration,* G. E. Hill, K. J. McGraw, Eds. (Harvard University Press, Cambridge MA, 2003).
17. A.I. Frenkel, G. V. Gorshin, *J. Synchrotron Rad.* **6,** 653-655 (1999)
18. S-F. Cheah, G. E. Brown Jr., G. A. Parks, *Am. Mineral.* **85**, 118-132 (2000).
19. G. R. Helz, J. M. Charnock, D. J. Vaughan, C.D. Garner, *Geochim. Cosmochim. Acta* **57**, 15-25 (1993).
20. E. Kaxiras, A. Tsolakidis, G. Zonios, S. Meng, *Phys. Rev. Lett.* **97**, 218102 (2006).
21. J. Stainsack *et al.*, *Inorg. Chim. Acta* **356**, 243-248 (2003).
22. J. M. Bowness, R. A. Morton, *Biochem. J.*, **51** (4), 530-535 (1952).
23. Y. Liu *et al.*, *Pigment Cell Res.* **17**, 262-269 (2004).
24. Y. Liu, J. D. Simon, *Pigment Cell Res.* **16**:72–80 (2003).
25. N. P. Edwards *et al.*, *Proc. Roy. Soc. London Ser. B* (doi: 10.1098/rspb.2011.0135).

Acknowledgments: Samples were provided by the Black Hills Institute Museum and the Museum für Naturkunde, Humboldt University, Berlin. We thank D. Schwarz-Wings for making the *Archaeopteryx* sample available. We also thank Perkin-Elmer, M. George, K. Palmer, E.

Kaxiras, V. Vishnyakov, and R. Morton for technical assistance and additional data, and D. Vaughan, G. Brown, and three reviewers for helpful comments on the manuscript. Portions of this research were carried out at SSRL, a national user facility operated by Stanford University on behalf of the U.S. Department of Energy, Office of Basic Energy Sciences. Funding was provided in part by an NERC Envirosync grant and by an anonymous private donor. R. Hartley provided the artist's drawing of *C. sanctus*. Data described in this paper are presented within the Supporting Online Material. **Author contributions:** RAW wrote the manuscript, analyzed the data, and supervised or assisted in all analyses. PLM co-wrote the manuscript and assisted in all analyses. HEB, NPE, and WIS assisted in all analyses and contributed to the manuscript. SMW performed the EXAFS analyses. KGT provided and supervised VP-FEG-SEM analyses. PLL provided specimen access and identification and also assisted with all X-ray measurements. PD consulted on the manuscript, and along with HY and LD assisted in field collection, preparation and identification of samples. UB supervised the SRS-XRF programme and assisted in manuscript preparation.

Supporting Online Material

www.sciencemag.org/cgi/content/full/science.1205748/DC1
Materials and Methods
SOM Text
Figs. S1 to S15
Tables S1 to S6
References

17 March 2011; accepted 2 June 2011
Published online 30 June 2011; 10.1126/science.1205748

Fig. 1. (**A**) *C. sanctus* (MGSF315), optical image. Yellow box shows detailed neck region discussed below. (**B** and **C**) SRS-XRF false color images of MGSF315 main slab and counterpart (Cu=Red, Ca=Blue, Zn=Green). (**D**) Neck region SRS-XRF false color image of a second *C. sanctus* (LL12418). Single element SRS-XRF maps of the main slab neck region of MGSF315 for (**E**) Ca, (**F**) Zn, and (**G**) S. (**H**) VP-FEG-SEM micrograph of possible eumelanosomes correlated with copper in the neck of MGSF315. (**I**) Artist's conception of eumelanin density in *C. Sanctus* based on the SRS-XRF images. Retrices in MGSF315 are folded; see white arrows in (**B** and **C**). White circles on (**C**) show SEM sample points.

Fig. 2. (**A**) Radial distribution functions (RDFs) from EXAFS analysis at the Cu Kα edge of two standards compared to fossil feathers. Red arrows in the copper oxide standard spectrum indicate features that are not present in the eumelanin standard. The *C. sanctus* and Green River fossil feathers give RDFs inconsistent with copper oxide or any other common mineral. (**B**) A comparison of the coordination chemistry of Cu in melanin to the fossil specimens (all distances to scale) showing similar coordination environments. (**C**) Proposed model for copper complexation in fossil melanin: Cu coordination from EXAFS for *C. sanctus* is superimposed onto an optimized computational model of melanin (*20*) showing how Cu may be accommodated into eumelanin.

Fig. 3. Top row (**A-G**) optical images, bottom row (**H-O**) SRS-XRF false color images of: (**A** and **H**) Green River fossil feather BHI-6358, (**B**, **I**, and **J)** Green River fossil feather and fish BHI-6319, (**C** and **K**) *G. yumenensis* fossil feather MGSF317, (**D** and **L**) eagle feather, (**E** and **M**) blue jay feather, (**F** and **N**) Hakel fossil squid BHI-2243B, (**G** and **O**) sectioned extant squid. (BHI-6358 and BHI-6319 Cu=Red, Ca=Green, Fe=Blue; MGSF317 Cu=Red, Ca=Green; remaining images are simply Cu=Red). All have copper zonation controlled by biological structure indicating eumelanin pigmentation.

Fig. 4. XANES spectra at the Cu Kα edge for three standards (thick black lines: copper metal foil, copper oxide, and natural melanin with high copper content) and six fossil specimens (*C. sanctus* neck [MGSF315], *A. lithographica* [MB.Av.100], three individual feather samples from the Green River Formation [BHI-6358, HMNS 2010.185.02, and BHI-6403]; and a fossilized squid ink sack from the Hakel Formation, *Sepia officinalis* [BHI-2243B], purple line). Arrows on the copper oxide spectrum indicate spectral features that do not appear on the eumelanin standard or on the fossils. Vertical dashed line indicates the fossils' average spectral maximum. Minimum organic copper content within the fossils as calculated by linear combination analysis is shown by values at right of each spectrum.

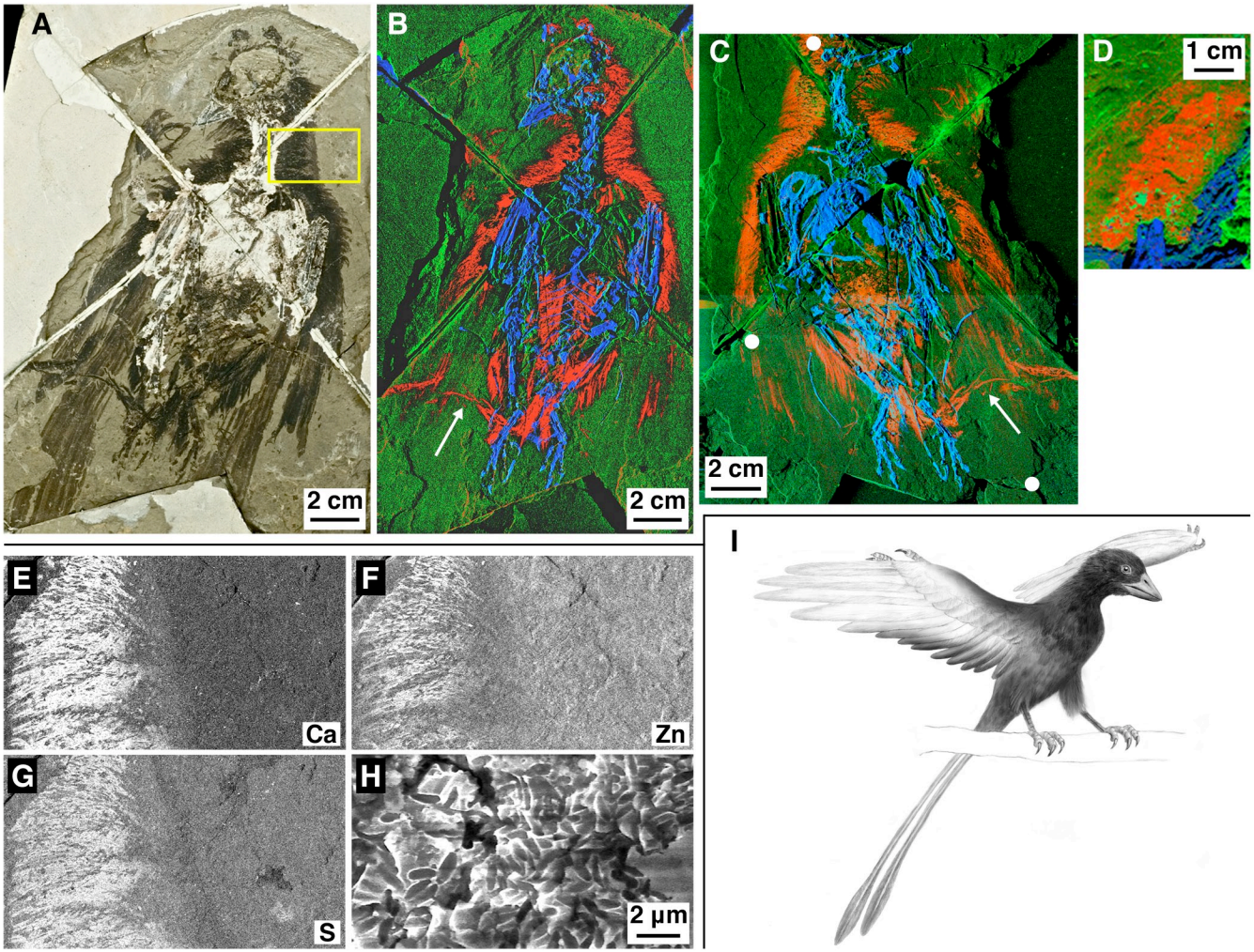
A
2 cm
B
2 cm
C
2 cm
D
1 cm
E
Ca
F
Zn
G
S
H
2 µm
I

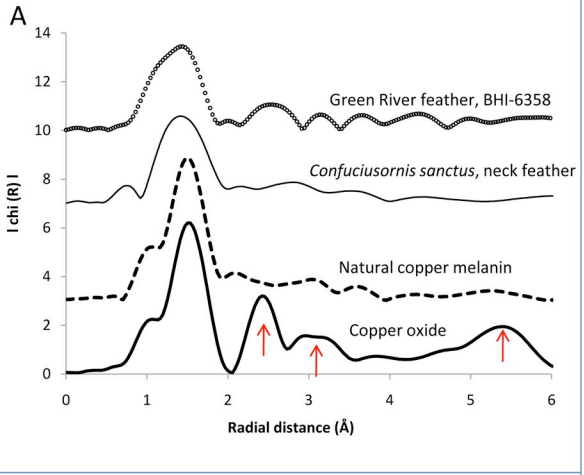
A
14
12
10
8
6
4
2
0
I chi (R) I
Green River feather, BHI-6358
Confuciusornis sanctus, neck feather
Natural copper melanin
Copper oxide
0
1
2
3
4
5
6
Radial distance (Å)

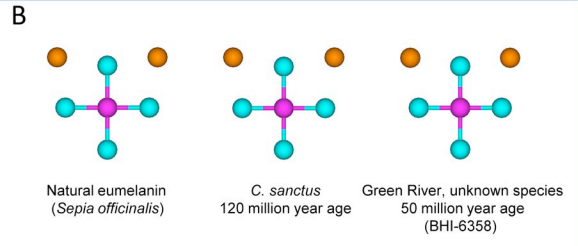
B
Natural eumelanin
(Sepia officinalis)
C. sanctus
120 million year age
Green River, unknown species
50 million year age
(BHI-6358)

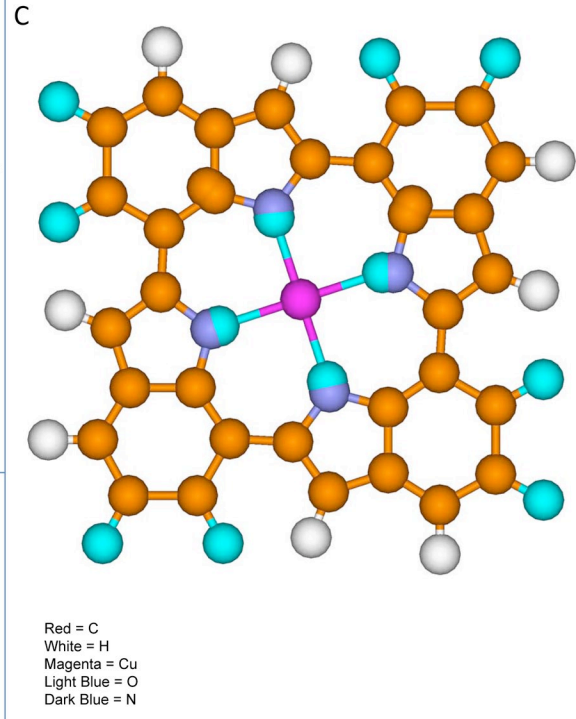
C
Red = C
White = H
Magenta = Cu
Light Blue = O
Dark Blue = N

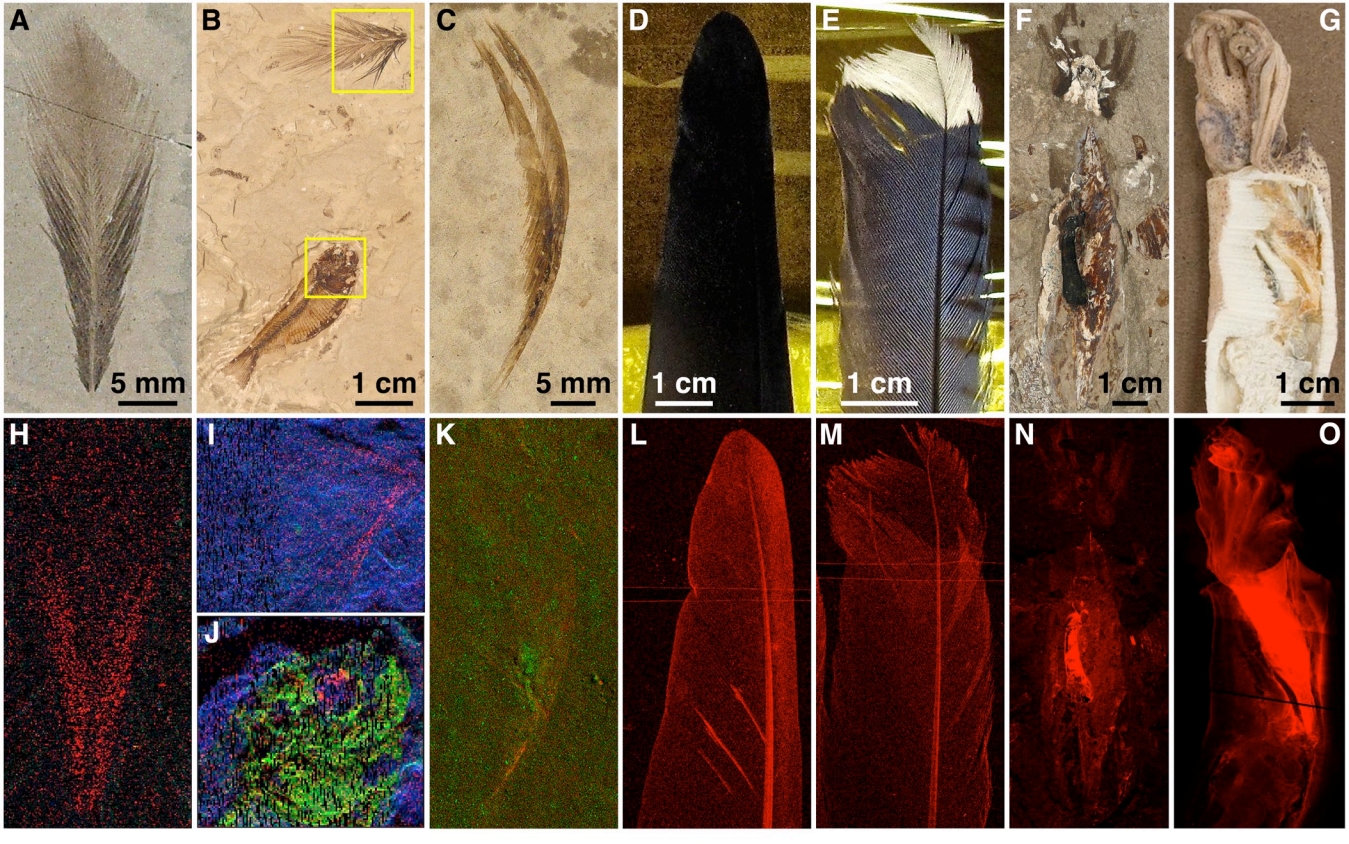
A
5 mm
B
1 cm
C
5 mm
D
1 cm
E
1 cm
F
1 cm
G
1 cm
H
I
J
K
L
M
N
O

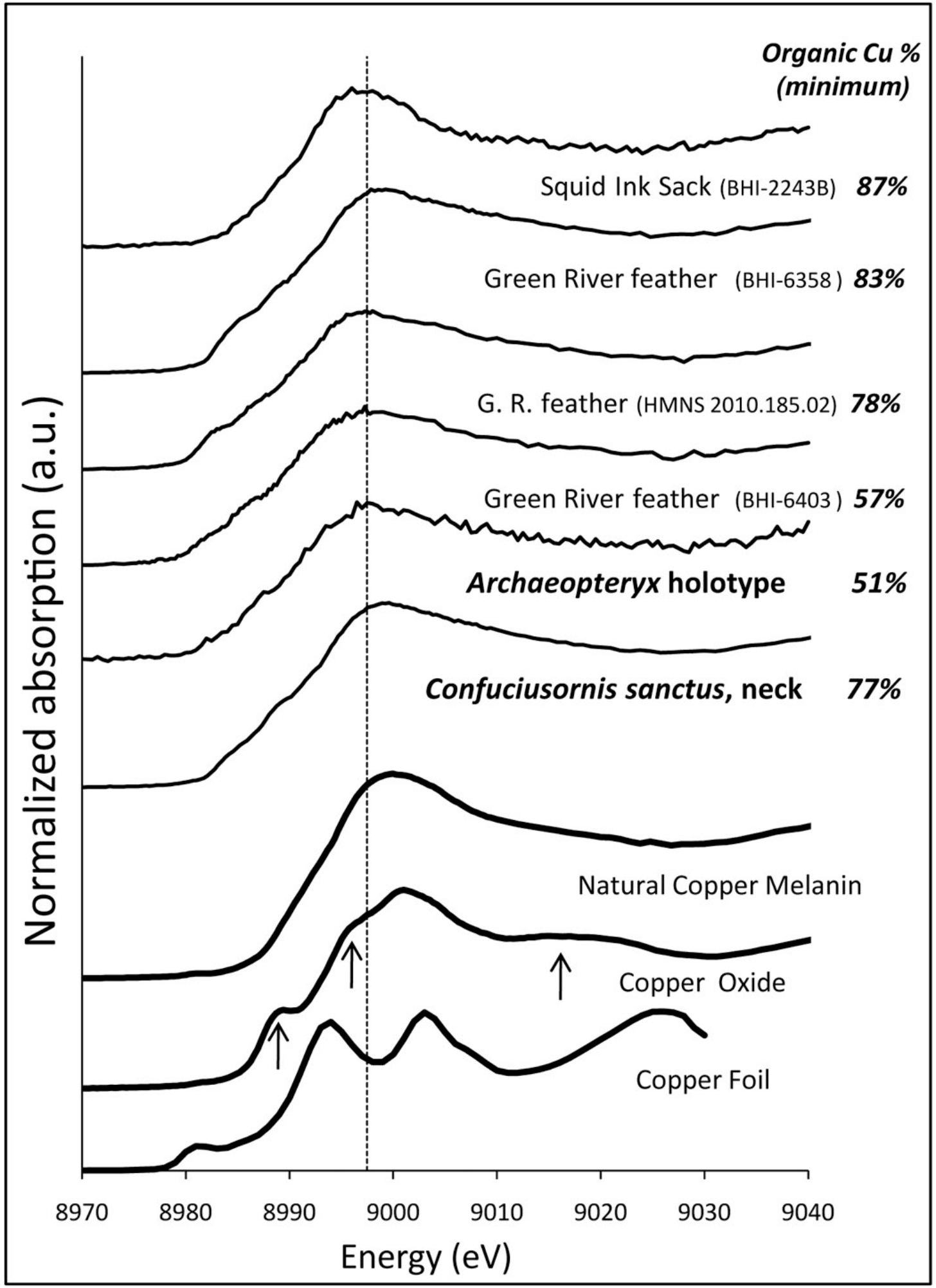
Organic Cu %
(minimum)
Squid Ink Sack (BHI-2243B) 87%
Green River feather (BHI-6358) 83%
G. R. feather (HMNS 2010.185.02) 78%
Green River feather (BHI-6403) 57%
Archaeopteryx holotype 51%
Confuciusornis sanctus, neck 77%
Natural Copper Melanin
Copper Oxide
Copper Foil
Normalized absorption (a.u.)
8970
8980
8990
9000
9010
9020
9030
9040
Energy (eV)